Evidence That Helix 8 of Rhodopsin Acts as a Membrane-Dependent Conformational Switch†

A. Gopala Krishna, Santosh T. Menon, Tracy J. Terry,‡ and Thomas P. Sakmar*

Laboratory of Molecular Biology and Biochemistry, Howard Hughes Medical Institute, The Rockefeller University, New York, New York 10021

Received January 10, 2002; Revised Manuscript Received April 30, 2002

ABSTRACT: The crystal structure of rhodopsin revealed a cytoplasmic helical segment (H8) extending from transmembrane (TM) helix seven to a pair of vicinal palmitoylated cysteine residues. We studied the structure of model peptides corresponding to H8 under a variety of conditions using steady-state fluorescence, fluorescence anisotropy, and circular dichroism spectroscopy. We find that H8 acts as a membrane-surface recognition domain, which adopts a helical structure only in the presence of membranes or membrane mimetics. The secondary structural properties of H8 further depend on membrane lipid composition with phosphatidylserine inducing helical structure. Fluorescence quenching experiments using brominated acyl chain phospholipids and vesicle leakage assays suggest that H8 lies within the membrane interfacial region where amino acid side chains can interact with phospholipid headgroups. We conclude that H8 in rhodopsin, in addition to its role in binding the G protein transducin, acts as a membrane-dependent conformational switch domain.

Rhodopsin, the rod cell photoreceptor, is probably the best studied G-protein-coupled receptor (GPCR[1]) and the only one to have been crystallized (Figure 1) (*1*). One of the novel features that emerged from the rhodopsin crystal structure was the helical conformation of the fourth cytoplasmic loop region. Termed helix-8 (H8), the fourth cytoplasmic loop begins at Asn^{310} and ends at membrane insertion of the palmitoyl groups attached to Cys^{322} and Cys^{323}. Among all of the GPCRs, only the family A receptors, of which rhodopsin is a prominent member, have a palmitoylation site and a putative H8 (*2*).

Structurally, rhodopsin exhibits "off" and "on" conformations. Absorption of light leads to the formation of an active meta II state of rhodopsin to which transducin (G_t) binds specifically. Movement of the transmembrane (TM) helices appears to be the major conformational change upon activation (*3*, *4*). Helix movements lead to exposure of regions of the protein otherwise buried in the membrane bilayer (*5*). Structural changes of the loop regions accompanying the movements of the TM helices play an important role in the off/on switch and lead to the specificity in rhodopsin−G_t interactions. Mutagenesis studies of specific amino acids in rhodopsin have shown the involvement of the second, third, and fourth cytoplasmic loops in both binding and activation of G_t (*6*−*10*).

One important implication of the helical conformation of H8 is the extension in the area occupied by the cytoplasmic face of rhodopsin. A one-to-one complex of rhodopsin and G_t proteins can be modeled, and the docking areas in the hypothetical complex appear to match (*11*, *12*). The conserved pattern of the amino acid residues in the fourth loop region among the family A GPCRs is additional evidence of the importance of H8 and its structure.

In an earlier report, we showed that H8 of rhodopsin plays an important role in modulating its interactions with G_t (*8*). Mutations of three amino acids (Asn−Lys−Gln) in the N-terminus of this loop led to a dramatic decrease in the ability of rhodopsin to activate G_t. In this study, we examine the structural properties of H8 and their implications to the function of rhodopsin. We used fluorescence and circular dichroism (CD) spectroscopy to show that H8 acts as a membrane surface recognition domain and that its structural properties are dependent on the lipid composition of the membrane. This novel amphitropic nature of H8 is in addition to its known involvement in G_t recognition. Our results support the notion that the fourth cytoplasmic loop has different conformations in the dark and light activated state of rhodopsin.

EXPERIMENTAL PROCEDURES

Buffers, hexyl agarose, 6-carboxyfluorescein (CF), sodium dodecyl sulfate (SDS), *n*-dodecyl-*β*-D-maltoside (DM), cetyltrimethylethylammonium bromide (CTAB), NP-40, 3[(3-cholamidopropyl)dimethylammonio]propanesulfonic acid (CHAPS), mellitin, and Triton X-100 were purchased from Sigma Chemical Co. (St. Louis, MO). Synthetic lipids 1,2-

† This research was supported in part by the Allene Reuss Memorial Trust. T.P.S. is an associate investigator of the Howard Hughes Medical Institute and a Senior Scholar of the Ellison Medical Research Foundation.

* To whom correspondence may be addressed. E-mail: sakmar@mail.rockefeller.edu. Mailing address: Rockefeller University, 1230 York Avenue, New York, NY 10021. Telephone: 212-327-8288. Facsimile: 212-327-7904.

‡ Present address: Department of Chemistry, Stanford University, Palo Alto, California.

[1] Abbreviations: CD, circular dichroism; CF, 6-carboxyfluorescein; cmc, critical micelle concentration; GPCR, G protein-coupled receptors; G_t, transducin; H8, helix 8; PS, phosphatidylserine; TFE, 2,2,2-trifluoroethanol; TM, transmembrane.

10.1021/bi025534m CCC: $22.00 © 2002 American Chemical Society
Published on Web 06/08/2002

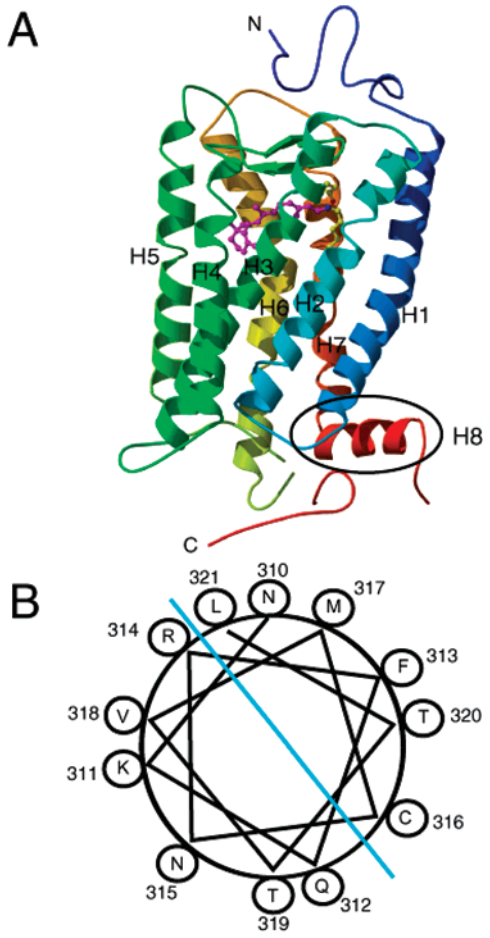

FIGURE 1: Secondary structure ribbon model (A) of rhodopsin. The molecule was generated using the crystal coordinates of the B chain of the published crystal structure (pdb 1F88). The N-terminus is toward the top and the C-terminus is toward the bottom of the figure. The seven TM helices are labeled H1−H7, and H8 is circled in black. H8 is oriented ~90° to the other helices and lies on the putative membrane surface. The figure was prepared with Molscript (*55*) and Raster3D (*56*). Panel B shows an Edmundson helical wheel projection of the H8 region. The hydrophobic and hydrophilic amino acids tend to cluster on opposite faces of the wheel, showing amphipathicity.

dioleoyl-*sn*-glycero-3-phosphocholine (DOPC), 1,2-dioleoyl-*sn*-glycero-3-phosphoethanolamine (DOPE), 1,2-dioleoyl-*sn*-glycero-3-phospho-L-serine (DOPS), dansyl-labeled DOPE, and dibromo lipids (6,7-dibromo-DOPC; 9,10-dibromo-DOPC, and 11,12-dibromo-DOPC) were all purchased as chloroform solutions from Avanti Polar Lipids (Alabastar, AL).

Peptide Synthesis. Peptides were synthesized by the Protein and DNA Technology Center at the Rockefeller University. All peptides were synthesized using F-moc amino acids and had amidated C-termini. Structures were confirmed by mass spectrometry. All peptides were purified to greater than 95% purity by reverse-phase high-performance liquid chromatography (RP-HPLC).

Preparation of Small Unilamellar Vesicles (SUVs) and Large Unilamellar Vesicles (LUVs). Lipids (16 mg/mL) from chloroform stocks were mixed in glass vials and dried by nitrogen evaporation followed by overnight storage under vacuum to remove residual chloroform. The lipids were hydrated in 250 μL of fluorescence buffer (10 mM Tris-HCl, pH 7.4, 100 mM NaCl, 2 mM $MgCl_2$) by vortexing. This lipid suspension was then subjected to sonication for 45 min in a Branson-1200 bath sonicator (Branson, CT). To prepare SUVs, the mixture was extruded through 50-nm pore polycarbonate membrane at least 19−21 times using LiposoFast Basic and Stabilizer (Avestin Inc., Ottawa, Canada). SUV size was confirmed to be in the 50−75 nm range by transmission electron microscopy. LUVs were prepared using membranes with a 100-nm pore size. Liposomes were used within 4−5 days of their preparation (DOPS vesicles were used within 2 days). Liposomes were always prepared by keeping the total lipid concentration at 20 mM irrespective of the lipid composition and diluted to the required concentration just before use. The vesicles were diluted 4-fold in fluorescence buffer before use. For CD experiments, the vesicles were prepared in the same fashion as above in 10 mM sodium phosphate buffer, pH 7.4, containing 25 mM NaCl.

Fluorescence Spectroscopy. All fluorescence measurements were carried out on a Spex fluorolog-τ3 fluorimeter (Jobin Yvon-Spex, NJ) equipped with a 450 W xenon arc lamp. All fluorescence studies were carried out in a 4 mm × 4 mm quartz cuvette. For intrinsic fluorescence studies of H8 and its analogue peptides, the sole phenylalanine residue was replaced by a tryptophan. In the liposome binding experiments, fluorescence emission spectra of the peptides were monitored from 310 to 450 nm while using a 295 nm excitation wavelength. Titrations were performed by addition of small aliquots (1−4 μL) of the liposome (stock concentration of 5 mM) to the peptide (1.25 μM in 0.4 mL). In all cases, blank spectra, containing either buffer alone or buffer containing micelles/vesicles, were subtracted from the final spectra.

Anisotropy values were measured in L-format and were calculated automatically using the software (Datamax) provided by the manufacturer according to the following equation:

$$r = (I_{vv} - I_{vh})/(I_{vv} + 2I_{vh}) \quad (1)$$

where r is the anisotropy of the sample, I_{vv} is the fluorescence of the sample detected when the excitation and emission polarizers are set at 90°, and I_{vh} is the fluorescence of the sample when the excitation polarizer is set to 90° and the emission polarizer is set to 0°. Readings at each titration point were recorded at least three times with a standard error less than 5%. Anisotropy measurements were used to determine the binding of the peptides to micelles or vesicles. Peptides were excited at 295 nm, and the anisotropy of their fluorescence was measured in the absence or presence of micelles/liposomes at 355 nm. Ludox was used as a standard in the anisotropy experiments (with an anisotropy value of ~0.97). Fluorescence resonance energy transfer (FRET) experiments were performed by exciting the tryptophan residue with 295-nm light and monitoring the dansyl fluorophore on the lipid by recording emission from 310 to 575 nm. The peptide concentration was kept constant at 1.25 μM while the concentration of the dansyl-labeled liposome varied from 0 to 115 μM. In all FRET experiments, acceptor (dansyl lipid) was always added to the donor (peptide) and not vice versa.

Efflux (Leakage) Measurements. The membrane leakage assay was done with LUVs loaded with the dye 6-carboxy-

fluorescein (CF) (Molecular Probes, OR) (*13*). All of the experiments were done with a liposome composition of DOPC/DOPS (1:1). Fluorescence buffer containing a 5-fold excess (relative to the amount of lipid) of CF was added to the lipid film, and sonication and extrusion were performed. Following extrusion, excess CF was removed by passing the suspension through a Micro Bio-spin P-30 spin chromatography column (Bio-Rad Laboratories, CA.). The release of CF from the liposomes induced by the binding of the peptides was followed at room temperature by monitoring the increase in fluorescence at 512 nm ($\lambda_{ex} = 430$ nm). Typically, to a 12.5 μM solution of liposomes (loaded with CF), 6 μM peptide was added, and fluorescence was monitored as a function of time. Fluorescence intensity in the absence of the peptide was considered as basal leakage, and 100% leakage was the fluorescence value after addition of 0.1% (v/v) of Triton X-100 indicating complete release of the probe. Mellitin was used as a model membrane-spanning peptide to confirm that the assay worked under our buffer conditions. Percentage leakage was calculated as $[(F - F_0)/(F_t - F_0)] \times 100$, where F and F_0 are the fluorescence intensities achieved in the presence and absence of the peptide and F_t is the fluorescence intensity achieved after the addition of Triton-X 100.

Quenching of Tryptophan Fluorescence by Brominated Lipids. Brominated phospholipids with bromines at stearoyl acyl carbon positions 6,7 or 9,10 or 11,12 were used to prepare SUVs. The fluorescence intensity of the H8 peptide was measured as a function of time at 355 nm ($\lambda_{ex} = 295$ nm) in samples prepared in lipid buffer alone, buffer containing unlabeled lipids, or SUVs of similar composition but containing 30% brominated phosphatidylcholine. Parallax analysis was used to calculate the depth of membrane insertion of the tryptophan residues on the peptide (*14*, *15*). The quenching efficiency is defined as $((\Delta F_0 - \Delta F) \times 100)/\Delta F_0$, where ΔF_0 and ΔF are the increase in fluorescence upon binding of the peptide to unlabeled vesicles and to liposomes containing brominated phospholipids, respectively. Distances between the tryptophan residue and bromines linked to the lipids were calculated using eq 2.

$$Z_{cf} = L_{ci} + \frac{(-1/(\pi C)) \ln F_1/F_2 - L_{21}^2}{2L_{21}} \qquad (2)$$

where Z_{cf} is the depth of the fluorophore from the center of the bilayer, L_{ci} is the distance from the shallow quencher to the center of the bilayer, L_{21} is the distance between both quenchers, and F_1 and F_2 are the fluorescence intensities of the fluorophore when incubated with membranes containing shallow and deep quencher, respectively. The parameter C represents the two-dimensional quencher concentration in the plane of the membrane in mole fraction of quencher lipid in total lipid per unit area. Here, $C = (0.3)/70$ Å^2, the average surface area per lipid molecule (*16*). The values for the constants were $L_{ci} = 11$ Å and $L_{21} = 6.5$ Å according to X-ray diffraction data (*17*).

CD Spectroscopy. Far-UV CD spectra of all of the peptides were recorded on an OLIS DSM CD spectrometer (Olis Inc., Bogart, GA) and analyzed on a Dell personal computer. All CD spectra were recorded in 10 mM sodium phosphate buffer, pH 7.4, containing 25 mM NaCl. Spectra were recorded from 250 to 190 nm in 1-nm steps with variable scan speed. The final spectra are averages of either four (for micellar system and TFE titration) or 60 individual spectra (in the presence of lipid vesicles). A 1-mm path length quartz cuvette was used, and all spectra were recorded at room temperature. For all measurements, a reference sample (also scanned an equal number of times) containing buffer, micelles, liposomes, or TFE was subtracted from the CD signal. Typically, 80 μM peptide was used in all of the CD studies although varying the concentration of the peptide did not affect the results. The final liposome concentration used in all of the cases was 5 mM. Molar ellipticity values were calculated according to the following expression: $[\theta] = (\theta/10)(115/(lc))$, where θ is the ellipiticity in millidegrees, 115 is the mean residue molecular weight in grams per mole, l is the path length in centimeters, and c is the concentration of the peptide in grams per liter. The value $[\theta]$ has the units of deg cm^2 dmol^{-1}.

Table 1: H8 Peptide Sequences

	sequence[a]											
peptide	310	311	312	313	314	315	316	317	318	319	320	321
H8	N	K	Q	F/W	R	N	C	M	V	T	T	L
H8-T				F/W	R	N	C	M	V	T	T	L
H8-M	S	P	D	F/W	R	N	C	M	V	T	T	L
H8-S	T	L	T	V	N	M	K	C	Q	N	F	R

[a] Amino acid numbering is from bovine rhodopsin sequence. Phe^{313} residue was substituted with a Trp residue for all fluorescence studies, including bromine-quenching experiments, while the wild-type peptide was used for other studies. H8, full-length wild-type peptide; H8-T, truncated peptide; H-8-M, modified peptide; and H8-S, scrambled peptide.

RESULTS

Peptide Design and Selection. To understand the structure−function relationship of the H8 region of rhodopsin, we chose to study the structural properties of peptides corresponding to that region. Amino acid sequences of three different peptides were chosen on the basis of the results of mutagenesis studies that we published previously (*8*). The sequences and their names have been shown in Table 1. The modified sequence was chosen because the "NKQ" to "SPD" mutation led to attenuation in transducin activation. The truncated version was chosen to elucidate the role of the first three amino acids of H8.

H8 Binding to SDS Micelles. For all intrinsic fluorescence studies, Phe^{313} in H8 was replaced by a tryptophan, which was used as the reporting group (Table 1). All three peptides (H8, H8-T, and H8-M) tested bound to SDS micelles, though to varying extents. Fluorescence anisotropy was measured as a function of SDS concentration (Figure 2A). The greatest increase of fluorescence anisotropy was seen for H8 peptide. The binding reached saturation at different SDS concentrations. H8 attained saturation between 1 and 2 mM SDS (under our experimental conditions, the critical micellar concentration (cmc) of SDS was ~1 mM). H8-T required a much higher micellar SDS concentration to attain saturation (~5 mM SDS). A microanalysis in the lower concentration range of SDS showed differences in the binding pattern. H8 showed possible cooperative binding to the SDS micelles, whereas H8-T and H8-M showed only a very small and linear increase of the anisotropy values (Figure 2, inset). Fluores-

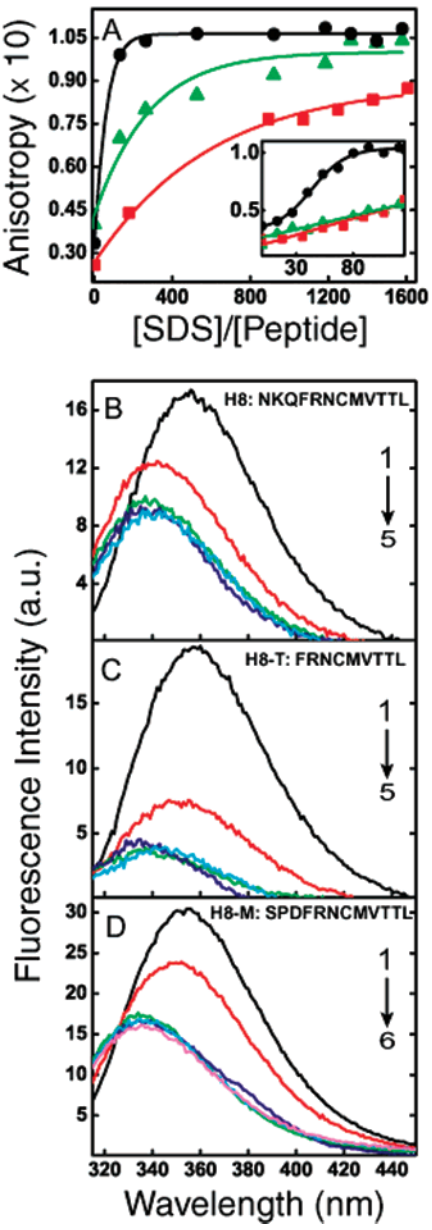

FIGURE 2: H8 fluorescence is affected upon binding to SDS micelles. (A) Binding of the peptides to SDS micelles was monitored by fluorescence anisotropy. The anisotropy of the tryptophan fluorescence from H8 (●, black), H8-M (▲, green) and H8-T (■, red) are shown as a function of SDS concentration. Concentration of the SDS stock used was 345 mM. The inset shows the titration of 1.2 μM H8 peptide with SDS of 69 mM stock concentration. At lower concentration of SDS H8 shows a cooperative nature of binding. Experiments were performed by exciting H8 peptide at 295 nm wavelength, and anisotropy was monitored at 355 nm. (B) The effect of increasing concentrations of SDS on the fluorescence spectral signature of H8. SDS concentrations are 0 (black, spectrum 1), 0.86 (red, 2), 2.6 (green, 3), 4.3 (blue, 4), and 12.9 mM (cyan, 5). (C) The effect of SDS on fluorescence signature of H8-T peptide. SDS concentrations are 0 (black, spectrum 1), 0.86 (red, 2), 2.6 (green, 3), 4.3 (blue, 4), and 12.9 mM (cyan, 5). (D) The effect of SDS concentrations on the fluorescence signal of H8-M peptide. Concentrations of SDS are 0 (black, spectrum 1), 1.72 (red, 2), 3.44 (green, 3), 5.16 (blue, 4), 6.88 (cyan, 5), and 8.6 mM (magenta, 6). All of the experiments were performed at room temperature. The fluorescence spectral signature did not change upon further increasing the SDS concentration. Fluorescence emission spectra of the peptides were recorded using an excitation wavelength of 295 nm. Peptide concentrations are all at 1.2 μM. Data shown are representative of several independent and reproducible experiments.

cence spectra of the peptides were also affected by binding to SDS. In all cases, there was a drop in the intensity and a dramatic blue shift of the λ_{max} of emission (Figure 2B,C,D). The effect saturated between 1 and 2 mM SDS. However, the percentage drop in fluorescence intensity and the degree to which the spectra shifted was different for the peptides. H8 and H8-M exhibited a 55% drop, and H8-T exhibited an 80% drop in intensity upon SDS addition. All three peptides showed a 15−18 nm blue shift upon saturation binding to SDS. H8-S peptide, wherein the amino acid sequence was scrambled, exhibited only a 10 nm blue shift and no significant change in its emission intensity (data not shown).

We also tested the effect of other detergents on the fluorescence of these peptides. DM, which has the same chain length as SDS but no charge, did not elicit any change in either the anisotropy or the emission signature of these peptides. CHAPS (zwitterionic) and NP-40 (nonionic) detergents also did not cause any change in the anisotropy or the fluorescence spectra of the peptides as a function of detergent concentration (data not shown). As an additional control, we also investigated the effect of the cationic detergent CTAB on the fluorescence of H8 peptide and its analogues (data not shown). The full length H8 peptide showed no change in its fluorescence signature with increasing concentrations of CTAB. Truncated H8 on the other hand showed an increase in its fluorescence (reverse of the effect seen with SDS), whereas the modified peptide showed a drop in its fluorescence upon addition of CTAB. H8 did not show any change in its λ_{max} of emission, while both H8-T and H8-M showed a small red shift (data not shown).

Secondary Structure Formation Upon Binding to SDS Micelles. SDS micelles have been often used as a membrane-mimetic model because they offer the advantage of extremely low levels of turbidity and light scattering (*18*, *19*). Induction of an ordered secondary structure in the peptides upon binding to SDS micelles was investigated by CD spectroscopy. CD spectra of all of the peptides were recorded in sodium phosphate buffer, pH. 7.4. In the absence of SDS, all three peptides (H8, H8-T, and H8-M) showed signatures corresponding to unordered structures with a negative peak in the 195−200 nm range (Figure 3A,B,C). With H8 and H8-M, increasing concentrations of SDS led to a loss of this peak and appearance of a positive peak in the 190−195 nm range and two new negative peaks at ∼208 and ∼222 nm (Figure 3A,C). Such a CD signature is typically obtained from a peptide existing in a helical conformation. At lower concentrations of SDS, H8 seemed to adopt a different structure. Addition of 2 mM SDS elicited a CD spectrum with a broad negative peak at 220 nm and a positive peak at 195 nm, generally seen with β-sheet structures (Figure 3A). This result prompted us to study the effect of lower SDS concentrations on the structure of H8. Only 200 μM SDS is sufficient to induce the formation of a β-sheet in H8 (Figure 3A, inset). H8-T on the other hand behaved very differently. As shown in Figure 3B, a negative CD signal in the 215 nm region and a positive peak in the 195 nm region were induced upon addition of SDS. The maximum helix formation by these peptides in SDS were 36%, 12%, and 33% for H8, H8-T, and H8-M, respectively, calculated according to Scholtz et al. (*20*).

H8 Binding to Membranes. To monitor the binding of H8 and its analogue peptides to membranes, we used both

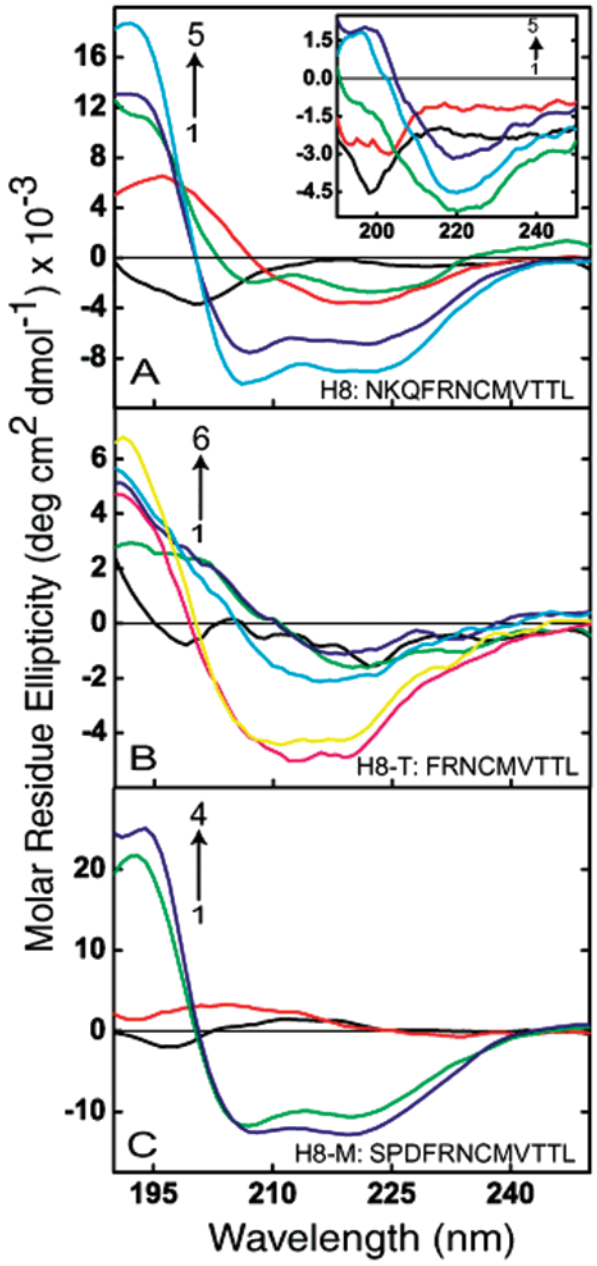

FIGURE 3: Ability of H8 to adopt secondary structure in membrane-mimicking environment depends on its sequence. CD spectra of H8 were recorded in increasing concentrations of SDS. Peptide concentration in each panel shown is 80 μM. All of the spectra shown are averages of four spectra and have been corrected for either buffer alone or buffer solutions containing an equivalent concentration of SDS. (A) CD spectra of H8 in the absence (black, spectrum 1) and presence of 2 (red, 2), 10 (green, 3), 14 (blue, 4), and 20 mM SDS (cyan, 5). The inset shows the titration of H8 peptide with 0 (black, spectrum 1), 40 (red, 2), 200 (green, 3), 280 (cyan, 4), and 400 μM SDS (blue, 5). (B) CD spectra of H8-T as a function of SDS concentration. SDS concentrations are 0 (black, spectrum 1), 10 (green, 2), 14 (blue, 4), 20 (cyan, 5), 36 (magenta, 3), and 72 mM (yellow, 6). (C) CD spectra of H8-M peptide as a function of SDS concentration. SDS concentrations are 0 (black, spectrum 1), 2 (red, 2), 10 (green, 3), and 14 mM (blue, 4). Spectra were recorded at room temperature, and the data shown are from a single experiment repeated several times with reproducible results. The striking difference in the spectral pattern of H8 and H8-T upon interaction with SDS shows the importance of the "Asn−Lys−Gln" tripeptide. Inability of H8-T to adopt helical structure shown in this figure and other structural data from the present work could be the reason for the attenuation in G_t activation caused by mutations in this region of rhodopsin (*8*).

fluorescence anisotropy and FRET. Liposomes were used as models for membrane binding studies. Experiments were performed by titration of the peptides (~1.25 μM) with small aliquots (1−2 μL) of 5 mM stock solutions of liposomes. Membrane binding was assessed using liposomes of various DOPC to DOPS ratios [DOPC, DOPC/DOPS (66:33), DOPC/DOPS (50:50), DOPC/DOPS (33:66), and DOPS]. Figure 4A shows the increase in anisotropy value of the fluorescence of the peptide upon binding to increasing concentration of the DOPC/DOPS (66:33) liposomes indicating that the peptide bound to the membranes. The fluorescence anisotropy value for H8 and H8-M dramatically increased from ~0.05 to ~0.2 and from ~0.05 to 0.15, respectively. H8-T on the other hand always showed a smaller rise compared with H8 indicating that it bound to membranes with much less affinity. Similar anisotropy patterns were observed with liposomes prepared with various lipid compositions (data not shown). Scattering artifacts in all of the anisotropy experiments were ruled out by the observation that increasing concentrations of liposome alone did not show any change in anisotropy value ($r = 0.03$).

Appearance of resonance energy transfer, a distance-dependent phenomenon, between two fluorophores has been extensively used to indicate association and binding (*21*). To monitor binding of H8 to membranes, we used tryptophan (in the peptide sequence) as the donor and a dansyl moiety (covalently linked to the phospholipid headgroup) as the acceptor. Titrations were performed by incremental addition (2−4 μL) of fluorescent liposomes (stock concentration of 5 mM) to a peptide solution (1.25 μM) in fluorescence buffer. Figure 4B shows the transfer of energy from the tryptophan to the dansyl fluorophore upon H8 binding to membranes. Upon excitation at 295 nm, there was a loss in intensity of the 355-nm peak (from tryptophan) and a concomitant rise of the 515-nm peak (from the dansyl moiety).

Surface Recognition Properties of the Peptide as Reported by Fluorescence Emission. Free H8 in solution displayed an emission maximum at 355 nm upon excitation at 295 nm (Figure 5). Extent of increase in fluorescence intensity and the blue shift of the membrane-bound peptide are both dependent on the lipid composition. Figure 5A shows that the fluorescence emission signature of H8 peptide was not affected upon binding to DOPC vesicles. Increasing amounts of DOPS in the liposome composition elicited both an increase in intensity and a blue shift of the wavelength of maximum emission (Figure 5B−D). Maximum rise in intensity and blue shift were seen in DOPS vesicles (~50% rise and a 17-nm blue shift, Figure 5D, inset). The fluorescence spectral signatures of H8-T upon binding to membranes of varying concentrations of DOPS were all similar with only very minor differences (data not shown). In all cases, a general drop in intensity accompanied with an invariant blue shift (~12 nm) was observed. Results with the modified peptide were similar to those with the truncated H8 peptide.

Ability of H8 Peptide to Adopt a Secondary Structure. Organic cosolvents have been extensively used to determine the inherent propensity of peptides to adopt a secondary structure. To determine the most favored secondary structure from the amino acid sequence of H8, we carried out CD spectroscopy in 2,2,2-trifluoroethanol (TFE)/water mixtures (Figure 6A). At low TFE concentrations, H8 peptide was in

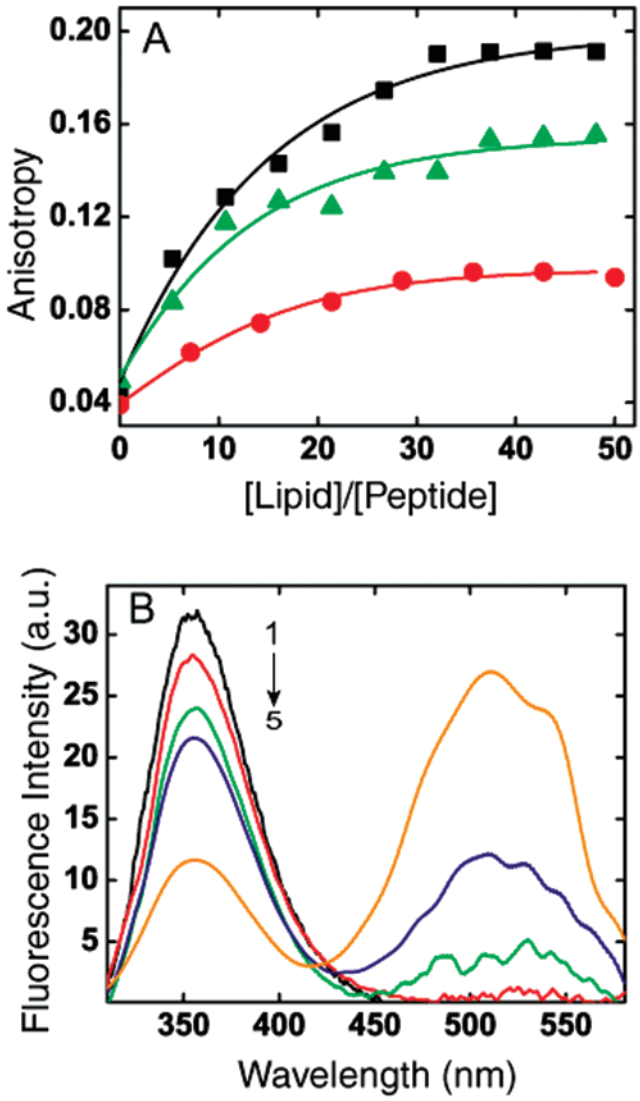

FIGURE 4: Membrane binding of H8 peptides. Binding of the H8 peptides to liposomes was monitored by fluorescence anisotropy and FRET. All of the H8 peptides bind to liposomes though with varying affinities. Anisotropy values were measured using an excitation wavelength of 295 nm and emission wavelength of 355 nm. Fluorescence emission spectra were recorded by exciting the peptide at 295 nm, and all of the spectra were corrected for either the buffer alone or equivalent amount of liposome. The concentration of the peptides used was 1.25 μM. (A) Anisotropy values of the H8 (black, ■), H8-M (green, ▲), and H8-T (red, ●) peptides as a function of liposome concentration. Concentration of the stock solution of liposome used in the titration was 5 mM. The composition of the liposome was DOPC/DOPS (33:66 mol % of each type of lipid). Each data point is an average of 3−5 readings with standard error less than 5% among them. (B) FRET was monitored from the tryptophan residue in H8 peptide to a dansyl fluorophore on the lipid headgroup. Liposome concentrations are 0 (black, spectrum 1), 3 (red, 2), 12 (green, 3), 25 (blue, 4), and 115 μM (orange, 5). For energy transfer experiments, 20 mol % of the DOPE used was fluorescently labeled with a dansyl fluorophore in a liposome composition of DOPC/DOPS/DOPE (45:10:45). Experiments were performed at room temperature. Data are from a single experiment that was reproducibly repeated several times for anisotropy and at least three times for FRET. The SEM for the anisotropy data were in the range of ±0.001. Anisotropy results with other lipososme compositions gave similar patterns among the three peptides though the extent of maximum increase in anisotropy increased with increasing mol % of DOPS. The K_d values for the peptides calculated from nonlinear regression analysis were 72, 36, and 53 μM for H8, H8-T, and H8-M, respectively.

an unordered form with a negative peak in the ~198/200 nm range, typical of a random coil structure. At and beyond 30% TFE, the negative peak in the 200 nm range disappeared and two negative peaks at 208 and 222 nm, and a positive peak in the range of 190 nm appeared, consistent with the peptide adopting a helical structure. The helicity of the peptide did not increase much beyond the 30% TFE concentration. Such a phenomena of maximum helix formation at 30% TFE has been reported for many peptides (*22*). Figure 6B shows the behavior of H8-T with increasing concentrations of TFE. In contrast to H8, H8-T did not adopt any secondary structure even at higher TFE concentrations. At all concentrations of TFE, the CD spectra showed a negative peak in the 195−200 nm region indicative of a random coil structure. In contrast, H8-M, wherein the first three amino acids were replaced with the "Ser−Pro−Asp" sequence, showed two negative peaks at 220 and 205 nm. In 100% TFE, the CD spectra had a single negative peak at 218 nm and a single positive peak at 192 nm (Figure 6C). Such a CD signature is indicative of the peptide adopting a sheetlike structure.

Secondary Structure of Membrane-Bound H8. The crystal structure of rhodopsin shows the H8 region in a helical conformation (*1*). On the other hand, the solution structure of a peptide corresponding to similar region shows a looplike structure (*23*). In an effort to clearly understand the structure of this domain of rhodopsin, we studied the behavior of H8 peptide and its analogues in the membrane-bound state. CD spectra of H8 peptide were recorded in both free form and membrane-bound form. Figure 7A shows the CD spectra of H8 in liposomes of various compositions. In buffer alone, all of the peptides showed a very prominent negative peak in the 195 nm range indicative of a random unordered structure. The inset in Figure 7A shows the spectrum of H8 bound to DOPC liposomes. Binding to zwitterionic DOPC did not induce any structure in H8, and the extent of unordered structure is increased greatly compared with buffer alone. Upon binding to membranes of increasing proportions of negatively charged DOPS, H8 adopted an ordered structure and the negative peak in the 200-nm region disappeared while two negative peaks at 210 and 222 nm and a positive peak in the 195-nm range gradually started to appear. At lower DOPS concentrations (DOPC/DOPS ratio of 66:33), the 195-nm negative peak was still prominently seen. In DOPC/DOPS ratios of 50:50 and 33:66, the best helical signatures are seen with defined peaks at ~222 nm and ~208 nm in addition to a large positive peak at 195 nm. In DOPS alone, the peptide did not show a very good helical signature. This indicates that the induction of helical structure in H8 is highly dependent on the PS content of the membranes. This result also confirms our observation from fluorescence data that the H8 peptide has the ability to recognize the surface charge on the membranes and switches its conformation in the membrane-bound form.

The truncated and modified peptides, H8-T and H8-M, essentially remained as random coils in the membrane-bound form, although in both the cases there was a hint of a sheetlike conformation existing to a small extent (from the negative peak in the 220-nm range) (Figure 7B,C). In both of these peptides, the sheetlike structure existed in the DOPC-bound form also, most probably as a consequence of nonspecific membrane association of these peptides.

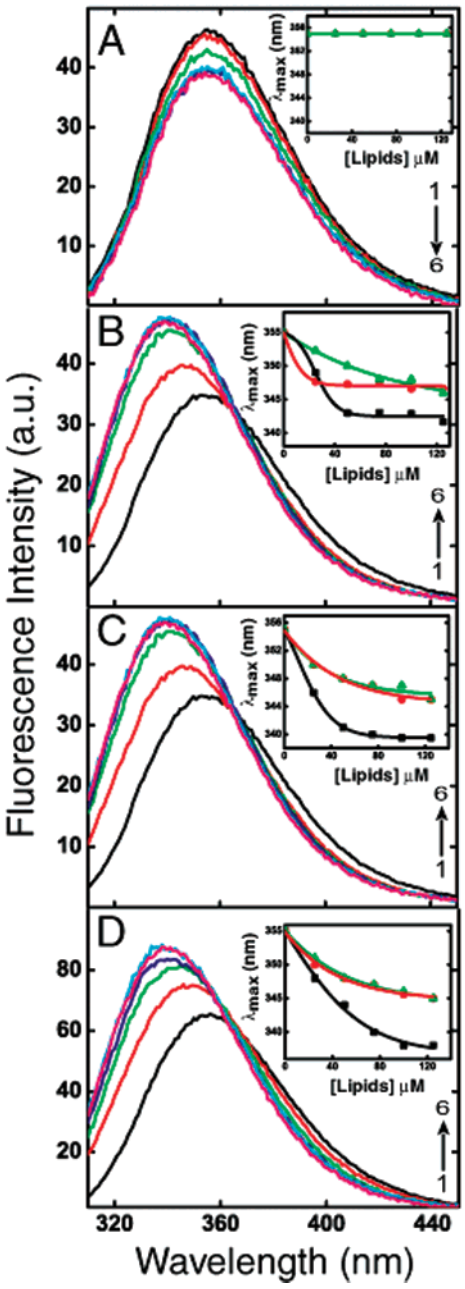

FIGURE 5: H8 is the membrane surface recognition domain in rhodopsin. The fluorescence spectral signature depends on the amount of DOPS in the liposome. Fluorescence emission spectra of H8 peptide were recorded by using an excitation of 295 nm. In all of the cases, the peptide concentration was 1.25 μM. (A) The change in fluorescence emission spectra of H8 with increasing concentration of DOPC liposomes. Concentrations of liposomes are 0 (black, spectrum 1), 25 (red, 2), 50 (green, 3), 75 (blue, 4), 100 (cyan, 5), and 125 μM (magenta, 6). The inset shows the change in fluorescence emission λ_{max} as a function of concentration of DOPC liposomes for H8 (black, ■), H8-M (green, ▲), and H8-T (red, ●). (B) The change in fluorescence emission spectra of H8 with increasing concentration of DOPC/DOPS (66:33) liposomes. Concentrations of liposomes are 0 (black, spectrum 1), 25 (red, 2), 50 (green, 3), 75 (blue, 4), 100 (cyan, 5), and 125 μM (magenta, 6). The inset shows the change in fluorescence emission λ_{max} as a function of concentration of DOPC/DOPS (66:33) liposomes for H8 (black, ■), H8-M (green, ▲), and H8-T (red, ●). (C) The change in fluorescence emission spectra of H8 with increasing concentration of DOPC/DOPS (33:66) liposomes. Concentrations of liposomes are 0 (black, spectrum 1), 25 (red, 2), 50 (green, 3), 75 (blue, 4), 100 (cyan, 5), and 125 μM (magenta, 6). The inset shows the change in fluorescence emission λ_{max} as a function of concentration of DOPC/DOPS (33:66) liposomes for H8 (black, ■), H8-M (green, ▲), and H8-T (red, ●). (D) shows the change in fluorescence emission spectra of H8 with increasing concentration of DOPS liposomes. Concentrations of liposomes are 0 (black, spectrum 1), 25 (red, 2), 50 (green, 3), 75 (blue, 4), 100 (cyan, 5), and 125 μM (magenta, 6). The inset shows the change in fluorescence emission λ_{max} as a function of concentration of DOPS liposomes for H8 (black, ■), H8-M (green, ▲), and H8-T (red, ●). The data shown are from a single experiment repeated several times with similar results. The changes in the fluorescence emission λ_{max} upon addition of the liposomes in different experiments are minimal ($\pm$1 nm). The fact that H8 shows larger shifts in the emission λ_{max} compared to H8-M and H8-T and that the latter two are not different from each other implicates the importance of the N-terminal three amino acids (Asn^{310}−Lys^{311}−Gln^{312}) in the H8 function.

Orientation of the Membrane-Bound H8. Membrane perturbation and changes in permeability can be extrapolated from the extent of release of an encapsulated dye from the interior of a liposome by a bound peptide. The ability of the peptide to induce dye release is dependent on its relative orientation in the bound form. Peptides that span across the membrane bilayer are referred to as pore-forming and hence cause more leakage of dye. On the other hand, peptides that bind only to the outer leaflet of the bilayer cause much less leakage of dye (*13*). Figure 8 shows the leakage of CF from liposomes caused by the binding of H8 peptides. The greatest release of CF was observed with the binding of the H8-T peptide (33%) and the least by H8-M peptide (25%). H8 by itself seemed to cause a moderate leakage (28%). We chose to compare H8 with its altered versions because in both of the other cases the formation of a secondary structure is uncoupled from the membrane-binding event. Differences in the extent of CF release by the three peptides indicates that mode of binding to membranes was different from each other.

Analysis of the Depth of Penetration of the Peptide Fluorophore. Quenching of fluorescence of the tryptophan fluorophore on the H8 peptides by quenchers covalently linked at various positions on lipid molecules can be used to measure the distance to which the fluorophore penetrates into the membrane. Brominated phospholipids, used as quenchers of tryptophan fluorescence, are good rulers for probing membrane insertion of peptides, because they act over a short distance and do not drastically perturb the membrane (*24*). Figure 9 shows that H8 was quenched maximally by the shallow quencher, whereas H8-T was quenched maximally by the deep quencher. Removal of the first three amino acids in the H8 peptides led to a loss of its surface active nature. Parallax analysis of the quenching data has been extensively used in membrane binding proteins and peptides (*14*, *15*). Mean distances obtained for the tryptophan

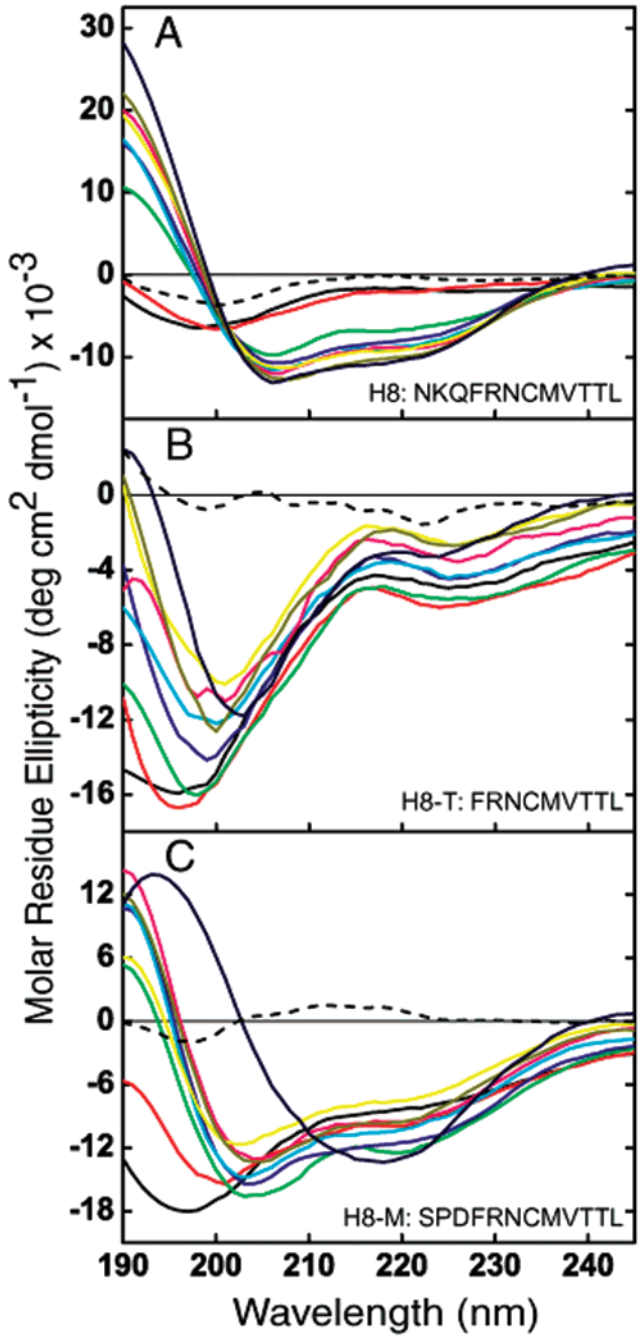

FIGURE 6: Secondary structure propensity of the H8 peptides. CD spectra of the H8 peptides were recorded as a function of TFE concentration. In the absence of TFE, the spectrum was recorded in 10 mM sodium phosphate buffer containing 25 mM NaCl. (A) The CD spectra of H8 peptide in the absence (black, dashed) or presence of 10% (black), 20% (red), 30% (green), 40% (blue), 50% (cyan), 60% (magenta), 70% (yellow), 80% (dark yellow), and 100% TFE (navy). (B) The effect of increasing concentrations of TFE on the CD spectra of H8-T. (C) The effect of increasing concentrations of TFE on the CD spectra of H8-M. Color codes of the spectra in panels B and C are the same as those in panel A. Peptide concentrations in all cases were maintained at 80 μM. Spectra shown are averages of five individual spectra and were recorded at room temperature.

residues of three peptides were 9.7 (±0.3) Å for H8, 10.2 (±0.17) Å for H8-M and 5.3 (±0.55) Å for H8-T from the center of the bilayer (the numbers in parentheses indicate the standard error of mean (n = 3)). It is clear that the tryptophan residue for the H8-T peptide is buried deep into

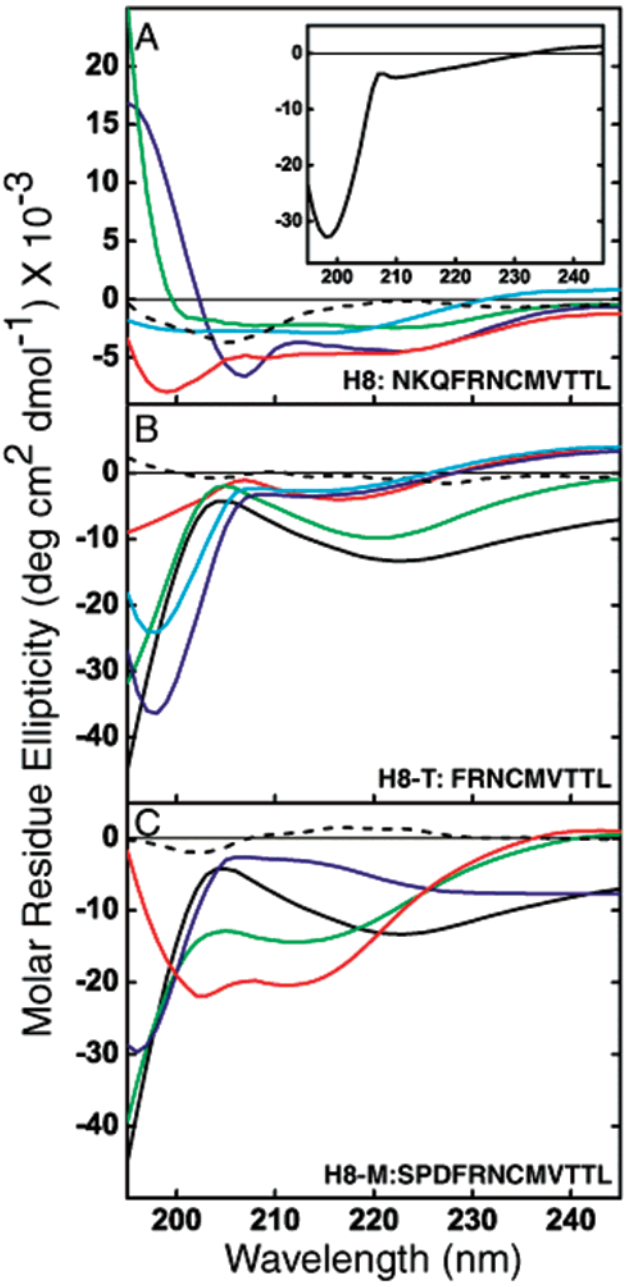

FIGURE 7: Membrane binding induces helix formation in H8. Far-UV CD spectra of H8 and its analogues were recorded to study the effect of membrane binding. (A) CD spectra of H8 peptide in the absence (black, dashed) or presence of DOPC/DOPS (66:33) (red), DOPC/DOPS (50:50) (green), DOPC/DOPS (33:66) (blue), and DOPS (cyan). The inset shows the CD spectra of H8 in the presence of DOPC. (B) CD spectra of H8-T peptide in the absence (black, dashed) or presence of DOPC (black), DOPC/DOPS (66:33) (red), DOPC/DOPS (50:50) (green), DOPC/DOPS (33:66) (blue), and DOPS (cyan). (C) CD spectra of H8-M peptide in the absence (black, dashed) or presence of DOPC (black), DOPC/DOPS (66:33) (red), DOPC/DOPS (50:50) (green), DOPC/DOPS (33:66) (blue), and DOPS (cyan). The peptide concentration in each panel is 80 μM, and the lipid concentration is 5 mM. All of the spectra are averages of 60 individual spectra and have been corrected for averages of 60 spectra of either buffer alone or buffer containing lipid. H8 adopts a helical conformation upon binding to membranes containing negatively charged phospholipids, whereas H8-T and H8-M do not exhibit such ability. The N-terminal three amino acids of H8 play an important role in its membrane recognition and inducing the helical conformation in the membrane-bound form. Data shown are representative of at least four independent and reproducible experiments.

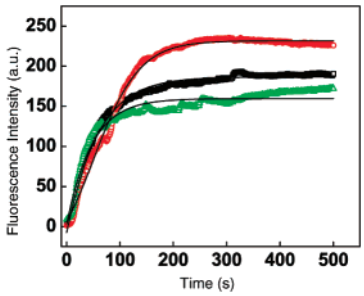

FIGURE 8: H8 is oriented parallel to putative membrane surface. Leakage of a dye entrapped in the liposomes is dependent on the orientation of the peptide in the bound form. Pore-forming peptides cause relatively large leakage compared to those that orient themselves parallel to the membrane. Fluorescence of the entrapped dye (CF) was monitored using an excitation wavelength of 430 nm and emission wavelength of 512 nm. Fluorescence data points represent leakage of the dye caused by H8 (black, □), H8-T (red, ○), and H8-M (green, △) as a function of time. Solid lines are sigmoidal fits of the data points (using Origin 6.1 graphing software). Larger leakage caused by H8-T means that the peptide is probably binding and is inserted deeper into the membrane.

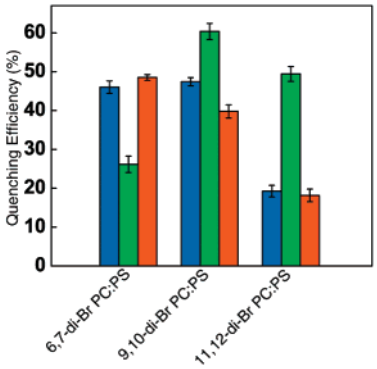

FIGURE 9: Quenching efficiency of the tryptophan fluorescence by brominated lipids. Tryptophan fluorescence was monitored by using an excitation wavelength of 295 nm and emission wavelength of 355 nm. Fluorescence was monitored as a function of time, and quenching was calculated as given in Experimental Procedures. Bars represent peptide H8 (blue), H8-T (green), and H8-M (orange). The tryptophan fluorescence of the full length H8 was maximally quenched by the shallow quencher suggesting that it lies parallel to the membrane surface. The tryptophan residue of the truncated version was quenched by the deep quencher because of its penetration into the bilayer. Although the modified peptide does not adopt a helical conformation, it still lies on the membrane surface, being quenched most by the shallow quencher.

the bilayer, whereas in case of H8-M and H8, it is closer to the surface.

DISCUSSION

One of the novel findings from the rhodopsin crystal structure was that its fourth cytoplasmic loop existed as an amphipathic helix oriented 90° to the other TM helices (*1*). In rhodopsin, H8 extends from Asn^{310} to Leu^{321} followed by two cysteines that have membrane-inserted palmitoyl groups attached by thioester linkages (*25*, *26*). Among all of the GPCRs, only the family A members clearly have a palmitoylation site that leads to the formation of an apparent analogue to H8. Extension of the area occupied by the cytoplasmic face of rhodopsin beyond the TM helices due to H8 has immense functional implications.

It is important to note that the crystal structure of rhodopsin represents its inactive conformation. Structural studies using various techniques have shown that rhodopsin undergoes large conformational changes upon activation (*27*). Several lines of evidence suggest that the H8 region in rhodopsin also undergoes structural changes upon activation. Whereas the crystal structure shows H8 to be in a helical conformation, solution structures of peptides corresponding to the H8 region using NMR have essentially shown this region to adopt a looplike structure (*23*). In the NMR structure (studied in detergent/membrane-free solutions), residues Asn^{310} through Gln^{312} appeared to be an extension of TM H7 and the region from Phe^{313} to Leu^{321} appeared to exist in a loopike conformation. Site-directed spin-labeling studies have shown a periodic behavior of properties of a spin label at amino acids Tyr^{306} to Arg^{314} (*28*). It was also shown that the side chains of three residues, Val^{318}, Thr^{320}, and Leu^{321}, were inaccessible to labeling, thereby suggesting that they are probably buried in the membrane bilayer. In the same study, the authors also report difficulty in assigning a specific structure to the region Asn^{315} to Leu^{321}. Spectroscopic probes covalently linked to Cys^{316} in rhodopsin report environmental changes upon its light-induced activation (*29*, *30*). These studies led to the possibility of the fourth cytoplasmic loop of rhodopsin existing in at least two different conformations and also the possibility that it switches from one to the other in a light-dependent manner. In earlier studies, we have shown the importance of this region in rhodopsin function (*8*, *9*). Modifications of the N-terminal tripeptide region (Asp^{310} to Gln^{312}) in H8 led to attenuation in rhodopsin's ability to activate G_t. Peptides corresponding to this region also showed a novel and interesting phenotype. The full-length peptide (from Asp^{310} to Leu^{321}) caused a change in the intrinsic fluorescence of the $G_{t\alpha}$ subunit and did not affect the fluorescence of $G_{t\beta\gamma}$. The modified peptide (in which the Asp−Lys−Gln region was replaced by Ser−Pro−Asp) did bind to the $G_{t\alpha}$ subunit and to G_t, but the extent of change in its fluorescence signature was only half as much as caused by the wild-type peptide. Truncated peptide (in which the first three amino acids, Asp−Lys−Gln, were deleted), on the other hand, did not bind G_t or its subunits. The fact that the conformation of the Asn^{310} to Leu^{322} region in the crystal structure does not agree with the solution NMR structure and also that a peptide of same sequence binds to $G_{t\alpha}$ in the absence of membranes or membrane-mimicking environments led us to study its structure−activity relationship in greater detail. Important insights were obtained by studying the membrane affinity of H8, its specificity to lipid composition in the membrane, its ability to adopt secondary structure, and its relative orientation in the membrane-bound form.

Many studies have reported the usefulness of detergents as membrane mimicking tools (*18*). Extensive studies using SDS micelles have shown that it is a very good probe to study the effects of membrane environment on the folding of proteins and peptides. SDS stabilizes various kinds of secondary structures below and above its cmc. Above its cmc, SDS has been shown to stabilize peptides in helical conformations (*31*−*33*), while below its cmc, SDS has been used in some cases to stabilize β-strands (*34*−*36*). Increasing anisotropy values of the fluorescence of the tryptophan residue in the H8 peptide confirm its binding to SDS micelles (Figure 2A). The blue shift of the emission λ_{max} also confirms that the tryptophan residue experiences a more hydrophobic environment in the micelle-bound form.

The fluorescence data unequivocally show the interaction of all three H8 peptides tested with SDS micelles. Although differences in the fluorescence spectral signatures among the three peptides are minimal, they show striking variability in their ability to adopt secondary structure upon binding to SDS. H8 peptide seems to show a dual behavior upon interaction with SDS. At lower SDS concentrations β-sheet types of structures are stabilized, whereas above its cmc, the peptide is stabilized in a α-helical conformation (Figure 3A and inset). The peptide exhibits a propensity to adopt both sheetlike and helical conformation with equal ease. This ability of the peptide to adopt two different types of conformations has great implications to its activity. It is possible that, in the receptor, H8 exhibits both conformations and each conformation represents either its inactive or active form (see below). The conformational switch is very specific to SDS and not observed in any other detergent. Such specificity also points to the dependence of the electrostatic interaction between the peptide and the membrane.

Although the truncated version of the peptide (in which the Asp−Lys−Gln tripeptide has been removed) binds to SDS, it does not adopt any secondary structure (Figure 3B). On the other hand, the modified H8 peptide, wherein the N-terminal tripeptide is replaced by Ser−Pro−Asp, adopts a helical structure upon binding to SDS but does not show a dual behavior like the H8 peptide (Figure 3C). These results point to the importance of the N-terminal three amino acids in controlling the structure−activity relationship of the peptide in the receptor. It is also important to remember that mutation of these three residues leads to a loss in the rhodopsin's ability to activate G_t and that the truncated peptide does not bind G_t. The helical structure of the H8 region probably plays a very important role in characterizing a specific conformation of rhodopsin.

Multifluorinated organic cosolvents have been used to study the secondary structural propensity of polypeptides. In particular, TFE has been shown to stabilize secondary structures in peptides for which the given amino acid sequence has the most propensity. TFE is known to induce and stabilize α-helices in sequences with intrinsic helical propensity and to induce β-turns and β-hairpins in other peptides (*37*, *38*). The TFE titration data show that H8 has the propensity to form a helix, and that removal of the N-terminal tripeptide region leads to a total loss of such propensity in the truncated H8 peptide. H8-T remains unordered under all conditions (Figure 6A,B). On the other hand, modifying the N-terminus of H8 leads to the formation of a β-sheet-like structure (Figure 6C).

These data, in addition to the SDS data, show the importance of the N-terminal tripeptide region in the receptor. This tripeptide sequence from amino acid 310 to 312 seems to be essential for the formation of the helical structure of H8. From the above results of TFE inducing different secondary structures in these peptides, it is clear that the first three amino acids in the H8 peptide play a significant role in the formation of a helical structure. Removal of Asn−Lys−Gln from the peptide leads to a total loss of the peptide's propensity to adopt any secondary structure, whereas changing it to "Ser−Pro−Asp" leads to the formation of a sheet and not a helical structure. These results strongly support the possibility of the Asn−Lys−Gln being a helix-nucleating domain for the H8 region in rhodopsin.

We propose that the Asn−Lys−Gln is the helix propagation site of H8 and plays a vital role in its structure−activity relationship. In rhodopsin, H8 is preceded by the highly conserved NPXXYXXX region. Despite its highly conserved nature in all of the rhodopsin family of GPCRs, the functional role of the NPXXY motif is still unclear. A similar domain (NPXY) has been implicated in being the internalization signal sequence in low-density lipoprotein receptor and in insulin-like growth factor-I receptor (*39*, *40*). Peptides corresponding to this region from the receptor have been shown to adopt a reverse-turn conformation (*41*). In other, independent studies, it has been shown that similar turnlike structures may play an important role in the earliest steps involved in initiation of protein folding (*42*, *43*). It has also been suggested that such sequences, though excellent candidates for protein folding initiation sites and observed in peptides or unfolded proteins need not necessarily be present in the final folded protein, even if they play a role in initiation of protein folding. Local structures formed during the earliest initiation events are necessarily unstable and, despite their importance in directing chain folding, could easily be eliminated from the final folded structure by subsequent folding events that make other conformations energetically more favorable (*42*, *43*).

The membrane interface region (IF), defined as the volume occupied by the headgroups of the lipids, has a strong ability to promote secondary structure formation in bound protein domains. Being the first accessible component of the bilayer, the interface plays a vital role in proper folding of the polypeptide chain. The interface region has been attributed as acting as a potent catalyst for formation of the secondary structure by the peptide (*44*). A great reduction in "per residue" free energy for the partitioning into the bilayer due to folding has been attributed as the biggest reason for this phenomenon. The "thermal thickness" of a single IF ($\sim$15 Å) has been proposed to readily accommodate an α-helix parallel to the membrane plane. Amphipathic α-helices, because of the oriented distribution of charged and hydrophobic amino acid residues on opposite sides, are used by many proteins as "membrane recognition" domains. Many proteins use amphipathic helices to sense changes in the physical properties of the bilayer such as electrostatic potential, lipid-packing density, or curvature strain and also to act as regulatory switches controlling the inactive or active state of the protein. These proteins that use α-helices as reversible and weak membrane anchors or membrane recognition domains have been classified as "amphitropic proteins" (*45*). In addition, it has also been suggested that membrane lipids themselves show specific chaperone-like activity and regulate protein folding (*46*). In rhodopsin, it is possible that H8 adopts its helical structure because of one or all of the above reasons.

The rod outer segment has a very unique membrane composition. As high as 50 mol % docosahexaenoyl phospholipids and a skewed distribution of PS (80% being present in the outer cytoplasmic layer) between the two layers of the membrane give it exceptional biophysical properties (*47*, *48*, *49*). Many of the photochemical functions of rhodopsin have been directly associated with physicochemical properties of the disk bilayer (*50*). Although H8 peptide binds to liposomes of almost any phospholipid composition, it does not always adopt helical structure. The helix-forming ability

of H8 is observed only in the presence of the acidic PS lipids. The fact that H8 binds to membranes of any lipid composition means that binding and folding are two independent phenomena. The hydrophobic amino acids probably aid in membrane binding and only the proper recognition of the charges leads to formation of the secondary structure.

The amount of helicity of H8 peptide increases until about 66 mol % of PS. Dependence of the helix formation of the H8 on the presence of PS correlates very well with the presence of more PS in the outer (cytoplasmic) leaflet of the rod disk membranes (*51*). The ability of H8 to exist as a helix depends on its primary structure also. Removal of three N-terminal charged residues (Asn−Lys−Gln) or its modification to another tripeptide sequence (Ser−Pro−Asp) to disrupt the charges leads to a loss of structure-forming ability by the peptide (Figure 6B,C). Though the truncated and the modified peptides bind to liposomes, they do not adopt secondary structure (Figure 7B,C). These results reiterate the fact that binding and folding are independent of each other. Another peptide in which the amino acid sequence has been scrambled also shows binding to liposomes but does not adopt structure (data not shown). It is quite possible that the H8 peptide with its net charge of +2 binds to negatively charged PS.

Orientation of the H8 in its membrane-bound form assumes great functional importance. Our results from "dye leakage" experiments and from the proximity of the tryptophan residue to quenchers covalently linked at various positions on the acyl chains of the lipids strongly support the hypothesis that H8 sits on the membrane surface, while the truncated version penetrates into the bilayer. These observations again reiterate the importance of the N-terminal tripeptide region. The charge orientation and the charge−charge interaction with the lipids probably hold the peptide on the membrane surface and do not allow its insertion into the bilayer. Additionally, the palmitoyl groups, covalently linked to the Cys^{322} and Cys^{323} of rhodopsin, may play a role in proper orientation of H8 on the membrane surface.

It is clear that the N-terminus of the H8 peptide is very crucial for both its structure and its function. Its role is not only to recognize $G_{t\alpha}$ but also to stabilize the helical conformation. Its specific binding to high -PS membranes also correlates with the physiological composition of the rod disk membranes with a skewed excess of PS in the cytoplasmic leaflet. Hessel et al. (*52*) recently reported the observation that the rod disk membrane phospholipids undergo a light-induced reorganization. They also reported that PS distribution is skewed because it is bound to rhodopsin and not available for extraction. Upon illumination with light, there is an increase in the extractable PS because it is released from rhodopsin.

We hypothesize that H8 is one of the PS binding sites of rhodopsin and remains in a helical conformation in the "off" state. Upon illumination, it loses its bound PS and adopts a looplike structure. Evidence of such a phenomenon of a specific lipid binding to rhodopsin and an alteration in its binding upon illumination has been shown previously by Beck et al. (*53*). In that report, though, they fail to specify the exact phospholipid involved. More recently, site-directed spin-labeling studies in the H8 region of rhodopsin have shown a light-dependent movement (2−4 Å) between Asn^{310} and Cys^{316} (*54*). Such an increase in distance between these two amino acids is possible only if the helix were to melt into a looplike structure. Using NMR, Yeagle et al. (*23*) have shown that in solution the H8 region actually exists as a loop and is not helical. The fact that H8 exists in a looplike conformation in low SDS concentration also suggests that it might switch conformation depending on its membrane environment. Studies are underway to define the precise role of palmitoylation and to determine whether the properties of H8 are general to family A GPCRs. For example, peptides from analogous regions of two other GPCRs, β-adrenoceptor from turkey erythrocytes and rat angiotensin II AT_{1A}, have been shown to adopt helical conformations (*55*, *56*).

ACKNOWLEDGMENT

We thank Dr. Richard DeSa (OLIS, Inc.), Dr. Ethan Marin, and Dr. Karim Fahmy.

REFERENCES

1. Palczewski, K., Kumasaka, T., Hori, T., Behnke, C. A., Motoshima, H., Fox, B. A., Le Trong, I., Teller, D. C., Okada, T., Stenkamp, R. E., Yamamoto, M., and Miyano, M. (2000) *Science 289*, 739−745.
2. Gether, U. (2000) *Endocr. Rev. 21*, 90−113.
3. Sheikh, S. P., Zvyaga, T. A., Lichtarge, O., Sakmar, T. P., and Bourne, H. R. (1996) *Nature 383*, 347−350.
4. Farrens, D. L., Altenbach, C., Yang, K., Hubbell, W. L., and Khorana, H. G. (1996) *Science 274*, 768−770.
5. Abdulaev, N. G., and Ridge, K. D. (1998) *Proc. Natl. Acad. Sci. U.S.A. 95*, 12854−12859.
6. Franke, R. R., Konig, B., Sakmar, T. P., Khorana, H. G., and Hofmann, K. P. (1990) *Science 250*, 123−125.
7. Franke, R. R., Sakmar, T. P., Graham, R. M., and Khorana, H. G. (1992) *J. Biol. Chem. 267*, 14767−14774.
8. Marin, E. P., Krishna, A. G., Zvyaga, T. A., Isele, J., Siebert, F., and Sakmar, T. P. (2000) *J. Biol. Chem. 275*, 1930−1936.
9. Ernst, O. P., Meyer, C. K., Marin, E. P., Henklein, P., Fu, W. Y., Sakmar, T. P., and Hofmann, K. P. (2000) *J. Biol. Chem. 275*, 1937−1943.
10. Fahmy, K., Sakmar, T. P., and Siebert, F. (2000) *Biochemistry 39*, 10607−10612.
11. Bourne, H. R., and Meng, E. C. (2000) *Science 289*, 733−734.
12. Sakmar, T. P., Menon, S. T., Marin, E. P., and Awad, E. (2002) *Annu. Rev. Biophys. Biomol. Struct. 31*, 443−484.
13. Donate, F., Yanez, A. J., Iriarte, A., and Martinez-Carrion, M. (2000) *J. Biol. Chem. 275*, 34147−34156.
14. Abrams, F. S., and London, E. (1992) *Biochemistry 31*, 5312−5322.
15. Ladokhin, A. S. (1999) *Biophys. J. 76*, 946−955.
16. Lewis, B. A., and Engelman, D. M. (1983) *J. Mol. Biol. 166*, 211−217.
17. McIntosh, T. J., and Holloway, P. W. (1987) *Biochemistry 26*, 1783−1788.
18. Garavito, R. M., and Ferguson-Miller, S. (2001) *J. Biol. Chem. 276*, 32403−32406.
19. Hoyt, D. W., Cyr, D. M., Gierasch, L. M., and Douglas, M. G. (1991) *J. Biol. Chem. 266*, 21693−21699.
20. Scholtz, J. M., Qian, H., York, E. J., Stewart, J. M., and Baldwin, R. L. (1991) *Biopolymers 31*, 1463−1470.
21. Lakowicz, J. R. (1999) *Principles of Fluorescence Spectroscopy*, 2nd ed., Kluwer Academic/Plenum Publishers, New York.
22. Hoyt, D. W., Cyr, D. M., Gierasch, L. M., and Douglas, M. G. (1991) *J. Biol. Chem. 266*, 21693−21699.
23. Yeagle, P. L., Choi, G., and Albert, A. D. (2001) *Biochemistry 40*, 11932−11937.
24. Bolen, E. J., and Holloway, P. W. (1990) *Biochemistry 29*, 9638−9643.
25. Papac, D. I., Thornburg, K. R., Bullesbach, E. E., Crouch, R. K., and Knapp, D. R. (1992) *J. Biol. Chem. 267*, 16889−16894.
26. Ovchinnikov, Y. A., Abdulaev, N. G., and Bogachuk, A. S. (1988) *FEBS Lett. 230*, 1−5.
27. Menon, S. T., Han, M., and Sakmar, T. P. (2001) *Physiol. Rev. 81*, 1659−1688.

28. Cai, K., Klein-Seetharaman, J., Farrens, D., Zhang, C., Altenbach, C., Hubbell, W. L., and Khorana, H. G. (1999) *Biochemistry 38*, 7925−7930.
29. Cai, K., Klein-Seetharaman, J., Farrens, D., Zhang, C., Altenbach, C., Hubbell, W. L., and Khorana, H. G. (1999) *Biochemistry 38*, 7925−7930.
30. Imamoto, Y., Kataoka, M., Tokunaga, F., and Palczewski, K. (2000) *Biochemistry 39*, 15225−15233.
31. Gierasch, L. M. (1989) *Biochemistry 28*, 923−930.
32. Mammi, S., and Peggion, E. (1990) *Biochemistry 29*, 5265−5269.
33. Rizo, J., Blanco, F. J., Kobe, B., Bruch, M. D., and Gierasch, L. M. (1993) *Biochemistry 32*, 4881−4894.
34. Wu, C. S., Hachimori, A., and Yang, J. T. (1982) *Biochemistry 21*, 4556−4562.
35. Zhong, L., and Johnson, W. C., Jr. (1992) *Proc. Natl. Acad. Sci. U.S.A. 89*, 4462−4465.
36. Waterhous, D. V., and Johnson, W. C., Jr. (1994) *Biochemistry 33*, 2121−2128.
37. Sonnichsen, F. D., Van Eyk, J. E., Hodges, R. S., and Sykes, B. D. (1992) *Biochemistry 31*, 8790−8798.
38. Searle, M. S., Zerella, R., Williams, D. H., and Packman, L. C. (1996) *Protein Eng. 9*, 559−565.
39. Hsu, D., Knudson, P. E., Zapf, A., Rolband, G. C., and Olefsky, J. M. (1994) *Endocrinology 134*, 744−750.
40. Chen, W. J., Goldstein, J. L., and Brown, M. S. (1990) *J. Biol. Chem. 265*, 3116−3123.
41. Bansal, A., and Gierasch, L. M. (1991) *Cell 67*, 1195−1201.
42. Wright, P. E., Dyson, H. J., and Lerner, R. A. (1988) *Biochemistry 27*, 7167−7175.
43. Dyson, H. J., and Wright, P. E. (1996) *Annu. Rev. Phys. Chem. 47*, 369−395.
44. White, S. H., Ladokhin, A. S., Jayasinghe, S., and Hristova, K. (2001) *J. Biol. Chem. 276*, 32395−32398.
45. Johnson, J. E., and Cornell, R. B. (1999) *Mol. Membr. Biol. 16*, 217−235.
46. Bogdanov, M., and Dowhan, W. (1999) *J. Biol. Chem. 274*, 36827−36830.
47. Brown, M. F. (1997) *Curr. Top. Membr. 44*, 285−356.
48. Hubbell, W. L. (1990) *Biophys. J. 57*, 99−108.
49. Crain, R. C., Marinetti, G. V., and O′Brien, D. F. (1978) *Biochemistry 17*, 4186−4192.
50. Brown, M. F. (1994) *Chem. Phys. Lipids 73*, 159−180.
51. Wu, G., and Hubbell, W. L. (1993) *Biochemistry 32*, 879−888.
52. Hessel, E., Muller, P., Herrmann, A., and Hofmann, K. P. (2001) *J. Biol. Chem. 276*, 2538−2543.
53. Beck, M., Siebert, F., and Sakmar, T. P. (1998) *FEBS Lett. 436*, 304−308.
54. Altenbach, C., Cai, K., Klein-Seetharaman, J., Khorana, H. G., and Hubbell, W. L. (2001) *Biochemistry 40*, 15483−15492.
55. Franzoni, L., Nicastro, G., Pertinhez, T. A., Tato, M., Nakaie, C. R., Paiva, A. C., Schreier, S., and Spisni, A. (1997) *J. Biol. Chem. 272*, 9734−9741.
56. Jung, H., Windhaber, R., Palm, D., and Schnackerz, K. D. (1996) *Biochemistry 35*, 6399−6405.
57. Kraulis, P. J. (1991) *J. Appl. Crystallogr. 24*, 946−950.
58. Merrit, E. A., and Bacon, D. J. (1997) *Methods Enzymol. 277*, 505−524.

BI025534M